EPSC Abstracts
Vol. 11, EPSC2017-766-1, 2017
European Planetary Science Congress 2017

Photometric properties of Occator's bright spots analogue materials

M. Ciarniello, S. De Angelis, C. Carli and M. C. De Sanctis
INAF-IAPS, Rome, Itay (mauro.ciarniello@iaps.inaf.it)

Abstract

We report about the photometric properties at visible wavelengths of powders of Occator's bright spots analogue materials, as inferred from laboratory measurements.

1. Introduction

The VIR (Visible and Infrared Spectrometer) experiment [1] onboard the Dawn mission [2] extensively observed the surface of the dwarf planet Ceres in the 0.2-5.1 µm wavelength range. The surface of Ceres is characterized by a low albedo (geometric albedo 0.094±0.007 [3]) and spectral modeling of VIR observations indicates that the global composition is dominated by serpentine, NH_4-phyllosilicates and carbonates mixed with dark materials [4]. Nonetheless, at small scale, albedo and compositional variability is observed in the form of "bright spots" [5], with a notable example represented by the Cerealia Facula in Occator crater, whose reflectance at standard geometry is 7-8 times larger than the surrounding terrains [6]. Spectral modeling of Occator's bright spots observations from VIR [6] indicates in these areas a large concentration of carbonates (up to 45–80 vol%) mixed with a dark material, phyllosilicates and minor amounts of ammonium-bearing species.

In order to complement the results from spectral modeling of remote sensing observations and to further characterize the physical properties of Occator's bright spots, laboratory measurements of the spectral and photometric properties in the VIS-NIR wavelength range of the identified end-members and their mixtures are needed. In this work, we focus on the photometric properties of these materials, as derived from spectrophotometric measurements performed with the spectro-goniometer in the SLAB facility, at IAPS-INAF, Rome.

2. Spectrogoniometer - setup

The reflectance spectra of powders were measured with a Fieldspec-Pro spectrophotometer mounted on a goniometer. The spectra were acquired between 0.35 and 2.50 µm, with 1 nm spectral sampling and 2-12 nm spectral resolution from the visible to the near IR. The source used was a QTH lamp. The illuminated spot was ca. 0.5 cm^2. The calibration of the spectrophotometer was performed with 99% Spectralon® optical standard (registered trademark of Labsphere, Inc.). The goniometer is PC-controlled and permit to vary incidence (inc) and emission (emi) angles in the principal scattering plane with phase angles (α) from 30° to 130°. The illumination and the detector instantaneous field of view cones are approximately 6° wide.

3. End-members and mixtures

The investigated materials are represented by: Natrite [Na_2CO_3], Ammonium Chloride [NH_4Cl], Illite [$K_{0.65}Al_2(Al_{0.65}Si_{3.35}O_{10}\ (OH)_2$], Magnetite [$Fe_3O_4$] and an intimate mixture ("bright spot mixture") of these end-members (50.5 %wt Natrite + 2.5%wt + 14%wt Illite +33%wt Magnetite). All the end-members and the mixtures have been prepared for various grain sizes ranges: <36 µm, 36-50 µm, 50-75 µm, 100-150 µm and 150-800 µm.

4. Measurements

We plan to measure reflectance spectra of single end-members and mixtures at various observation geometries in the principal scattering plane with incidence and emission angles ranging in the 0°-65° interval and phase angles from 30° to 90°.

5. Preliminary results

In Fig. 1 the reflectance factor (REFF) at 0.7 µm for the single end-members and the "bright spot mixture" at grain size <36 µm is reported as a function of the incidence and emission angles respectively. Natrite (nat1) and Ammonium Chloride (cla1) show the highest albedos of the samples while magnetite (mgt1) is characterized by a very low reflectance. The reflectance level of the "bright spot mixture" is ~0.2 at inc =30°, emi=0°, α=30° slightly lower than the value derived from VIR measurements at 0.55 µm (I/F=0.26 corresponding to REFF = 0.3). The REFF curves are not exactly symmetrical for inc-emi exchange, possibly due to residual systematics error in the measurements.

In Fig. 2 the REFF curves of the "bright spot mixture" and Illite (imt2) are shown as a function of the phase angle for specular observation geometries (inc = emi). It can be noticed that while the Illite sample exhibits an isotropic scattering behavior, the "bright spot mixture" appears relatively forward-scattering.

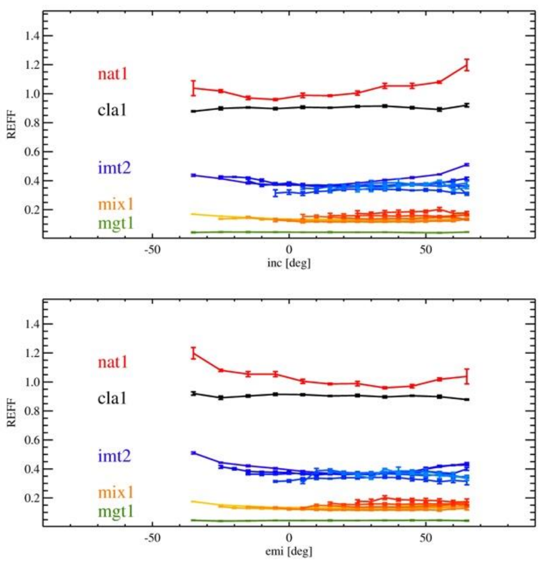

Figure 1. REFF curves at 0.7 µm as a function of incidence (top panel) and emission (bottom panel) angles for Natrite (nat1), Ammonium Cloride (cla1), Illite (imt2), Magnetite (mgt1) and bright spot mixture (mix1). The sign of the incidence and emission angles discriminate between opposite positions in the principal scattering plane with respect to the normal at the sample plane. Incidence and emission directions in the same semi-plane have opposite signs. Phase angle α=inc+emi is 30°. Different colored curves for imt2 and mix1 correspond to different phase angles (from 30° to 90°) (Figure 2).

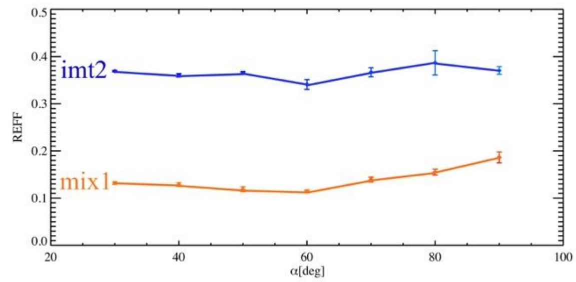

Figure 2. REFF curves at 0.7 µm as a function of phase angle (α) for Illite (imt2), and "bright spot mixture" (mix1) for specular observation geometries (inc=emi).

6. Summary

REFF curves for the materials and the observation geometries described in Sec. 3 will be measured, allowing us to characterize the photometric behavior of single end-members and mixtures. Along with this, the effect of the grain size on the photometric properties of the end-members and their mixtures will be investigated. Comparison of these measurements with the photometric properties of Occator's bright spots as derived from Dawn remote sensing instruments (VIR, FC) will provide further insights on the physical properties of the regolith.

Acknowledgements

This work is supported by an Italian Space Agency (ASI) grant.

References

[1] De Sanctis et al. 2011, Space Sci. Rev., 163, 329.

[2] Russell, C. T., & Raymond, C. A. 2011, Space Sci. Rev., 163, 3.

[3] Ciarniello et al., 2017, A&A, 598, A130.

[4] De Sanctis et al., 2015, Nature, 528, 241.

[5] Palomba et., 2017, Icarus, submitted.

[6] De Sanctis et al., 2016, Nature, 536, 54.